

## Significant improvement in planetary system simulations from statistical averaging

David M. Hernandez,<sup>1</sup> Eric Agol,<sup>2</sup> Matthew J. Holman,<sup>1</sup> and Sam Hadden<sup>1</sup>

<sup>1</sup>*Harvard-Smithsonian Center for Astrophysics*

<sup>2</sup>*Astronomy Department, University of Washington*

### ABSTRACT

Symplectic integrators are widely used for the study of planetary dynamics and other  $N$ -body problems. In a study of the outer Solar system, we demonstrate that individual symplectic integrations can yield biased errors in the semi-major axes and possibly other orbital elements. The bias is resolved by studying an ensemble of initial conditions of the outer Solar system. Such statistical sampling could significantly improve measurement of planetary system properties like their secular frequencies. We also compared the distributions of action-like variables between high and low accuracy integrations; traditional statistical metrics are unable to distinguish the distribution functions.

*Keywords:* Computational methods — Celestial mechanics — Exoplanet dynamics — Galaxy dynamics

Symplectic maps (Hairer et al. 2006) are well suited for studying the astrophysical  $N$ -body problem; they have been used to study the evolution of our Solar system and exoplanetary systems (e.g., Wisdom & Holman 1991). In this note, we show that an application of a symplectic integrator, regardless of its time step or order, can give biased errors and trajectories. This bias can be mitigated by considering a statistical sample of trajectories.

Consider the problem of the Sun plus the four giant planets. The bodies are treated as point particles obeying Newtonian gravity. We integrate this system for 10,000 years using the symplectic Wisdom–Holman map (WH) in canonical Democratic Heliocentric coordinates (Wisdom & Holman 1991; Duncan et al. 1998). If  $h$  is the timestep and  $\epsilon$  is the ratio of the maximum planetary mass to the Solar mass, the error scales as  $\mathcal{O}(\epsilon h^2)$ <sup>1</sup>. As a function of phase space coordinates, the  $N$ -body Hamiltonian is,

$$H = \sum_i \frac{\vec{P}_i^2}{2m_i} - \frac{Gm_0m_i}{Q_i} + \frac{1}{2m_0} \left( \sum_{i \neq 0} \vec{P}_i \right)^2 - \sum_{0 < i < j} \frac{Gm_im_j}{Q_{ij}}, \quad (1)$$

while the error in the Hamiltonian is (Hernandez & Dehnen 2017),

$$\begin{aligned} H_{\text{err}} = & \frac{h^2}{24} \left( -\frac{1}{m_0} \left( \sum_{i \neq 0} \frac{Gm_0m_i}{Q_i^3} \vec{Q}_i \right)^2 - \sum_{0 < i < j} \frac{Gm_im_j}{Q_{ij}^5} \left[ V_{ij}^2 Q_{ij}^2 - 3(\vec{V}_{ij} \cdot \vec{Q}_{ij})^2 \right] + \sum_{\substack{i,j > 0 \\ i \neq j}} \frac{G^2 m_0 m_i m_j}{Q_{ij}^3 Q_i^3} \vec{Q}_{ij} \cdot \vec{Q}_i \right. \\ & \left. + \sum_{i \neq 0} \left( \frac{G}{Q_i^5} \left[ (\vec{P}_\odot \cdot \vec{P}_i) Q_i^2 - 3(\vec{P}_\odot \cdot \vec{Q}_i)(\vec{P}_i \cdot \vec{Q}_i) \right] + \frac{2Gm_i}{m_0 Q_i^5} \left[ P_\odot^2 Q_i^2 - 3(\vec{P}_\odot \cdot \vec{Q}_i)^2 \right] + \frac{2}{m_i} \left( \sum_{j \neq 0, i} \frac{Gm_im_j}{Q_{ij}^3} \vec{Q}_{ij} \right)^2 \right) \right) \\ & + \mathcal{O}(h^4). \end{aligned} \quad (2)$$

Corresponding author: David M. Hernandez  
dmhernandez@cfa.harvard.edu

<sup>1</sup> Hernandez & Dehnen (2017) used a different error convention for which the scalings in this paper are multiplied by  $\epsilon$ .

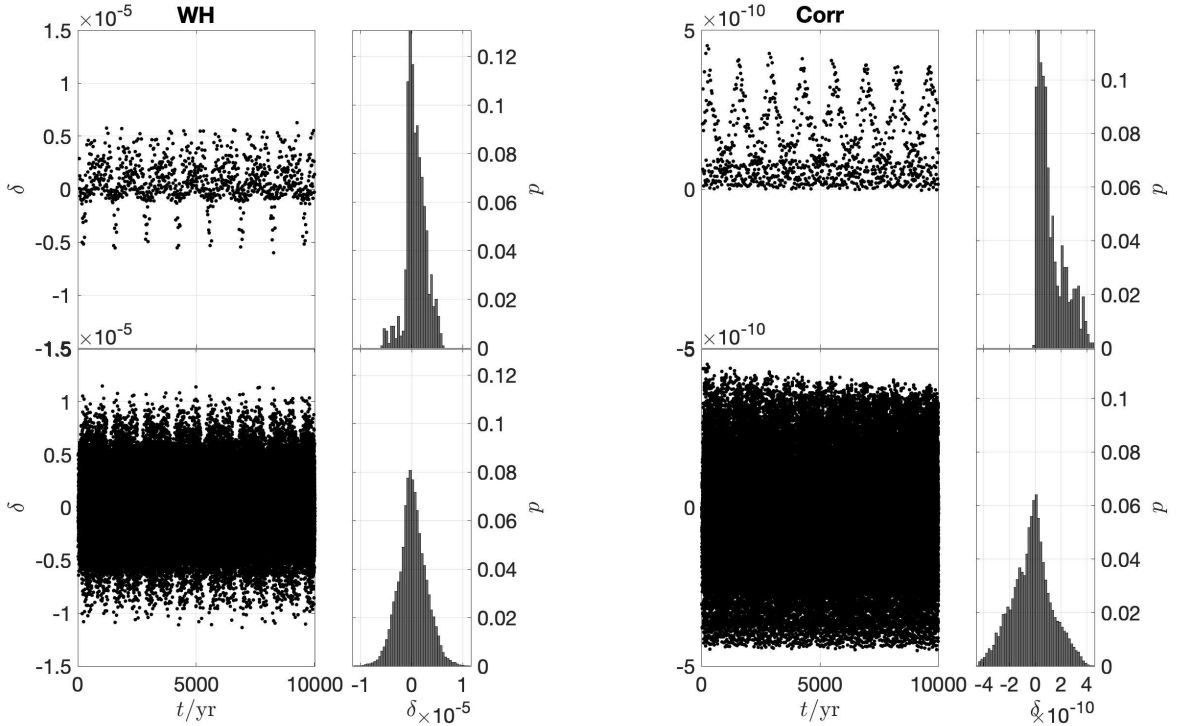


**Figure 1.** Errors,  $\delta$ , in integrations of the outer Solar system. The four left panels show integrations using WH with  $h = 1$  yr. The four right panels show integrations using WH with a 17th order corrector and  $h = 0.01$  yrs. The top panels show one initial condition. The bottom panels show the results for 100 initial conditions; the starting phase for each integration has been chosen randomly. While the top panels show biased mean energies, the bottom panels mitigate this bias.

Here,  $G$  is the gravitational constant,  $\vec{Q}_i$  and  $\vec{P}_i$  are the  $i$ th canonical coordinate vectors,  $m_i$  is the  $i$ th mass,  $\vec{V}_i = \vec{P}_i/m_i$ , and  $\vec{P}_\odot = \sum_{j \neq 0} \vec{P}_j$ .  $\vec{V}_{ij} = \vec{V}_i - \vec{V}_j$  and  $\vec{Q}_{ij} = \vec{Q}_i - \vec{Q}_j$ . Some terms in eq. (2) scale as  $\epsilon$  and are dominant while others scale as  $\epsilon^2$ .

We choose  $h = 1$  yr and generated output every 10 years. The initial conditions are at a time randomly chosen between 0 to 100 yrs,  $t_{\text{start}}$ . To obtain the initial conditions, we run WH with 17th order symplectic correctors (Wisdom et al. 1996) and  $h = 0.005$  yr from time 0 to  $t_{\text{start}}$  (we apply a corrector to the initial conditions and an inverse corrector on output). Integrating in this way from 0 to 100 yrs gives energy error  $\delta = \Delta H/H = 1.9 \times 10^{-13}$ , close to the limit from rounding errors.

The top left panel in Fig. 1 displays  $\delta$  over the 10,000 yrs. The error is not symmetric about 0, indicating a trajectory with biased errors. This is confirmed with the adjacent histogram of the errors. The mean  $\delta$ ,  $\bar{\delta}$ , is  $8.2 \times 10^{-7}$ . This curve is described exactly by the Hamiltonian,

$$\tilde{H} = H + H_{\text{err}}. \quad (3)$$

Note  $\tilde{H}$ , not  $H$ , is conserved by the mapping, as can be confirmed numerically (Hernandez & Dehnen 2017).

Next, we perform an additional 99 experiments. These are identical to the first except that  $t_{\text{start}}$  is chosen randomly each time. The results of the combined 100 experiments are plotted in the bottom left panel of Fig. 1. The errors are more symmetric about 0, resulting in  $\bar{\delta} = 1.5 \times 10^{-7}$ , which is 5.4 times smaller. We find evidence that  $\bar{\delta}$  is 0 as the number of initial conditions tends to  $\infty$ . For 10,000 initial conditions,  $\bar{\delta} = -7.5 \times 10^{-9}$ , consistent with a standard error scaling as  $n^{-1/2}$ , and a population  $\bar{\delta} = 0$ , where  $n$  is the number of initial conditions.

The adjacent plot shows a histogram that is approximately normally distributed around 0 with skewness of 0.042. This skewness was not improved by using the 10,000 initial conditions or by allowing  $t_{\text{start}}$  to take values between 0 and 1,000 years, to capture secular frequency timescales.

Our experiment demonstrates that the trajectories of a symplectic integrator depend on the initial phase, which is undesired. We can understand this by noting that the initial phases are found by solving  $\tilde{H}$  which, in turn, changes the value of  $\tilde{H}$ . The subsequent evolution of  $H$  from the mapping depends on the initial  $\tilde{H}$ . At leading order in  $\epsilon$ , the energy error is a weighted sum of the semi-major axes errors, so a biased energy error implies at least one biased semi-major axis error. Biases in other action-like variables may also exist.

Our averaging procedure improved the distribution of errors. Such averaging procedures could have a significant impact, for instance, in improving calculation of secular frequencies in the Solar System (Laskar et al. 2011).

Substantial effort has been invested into higher accuracy symplectic integrators (Yoshida 1990; Wisdom et al. 1996; Laskar & Robutel 2001; Blanes et al. 2013; Rein et al. 2019). We investigate also their biases, using WH with a 17th order symplectic corrector. The error scales as  $\mathcal{O}(\epsilon h^{18}) + \mathcal{O}(\epsilon^2 h^2)$ . The integration time remains the same; output is generated every 10 yrs, and the timestep is  $h = 0.1$  yrs. The right panels of Fig. 1 show the results for one and 100 initial conditions, respectively. Again, histograms of the errors are also shown. The error is dominated by the  $\mathcal{O}(\epsilon^2 h^2)$  term. Compared to the low accuracy experiments, the order in the error has changed by  $\epsilon(0.1)^2 = 10^{-5}$ , explaining the change in scale. This is a factor  $\epsilon$  smaller than if we had just reduced the time step. Our goal is to reduce the error, which we have done by using a smaller step and symplectic correctors, but other ways of reducing error exist.

For one initial condition, the error is again not symmetric about 0, and  $\bar{\delta} = 1.2 \times 10^{-10}$ . When the 100 initial conditions are studied,  $|\bar{\delta}|$  decreases by a factor 5.0;  $\bar{\delta}$  is now  $-2.5 \times 10^{-11}$ . The errors are approximately normally distributed around 0 with skewness of 0.022. An ensemble of initial conditions again improved bias for higher accuracy methods.

Using standard statistical tools to distinguish action-like variables between the low and high accuracy integrations is not helpful. We computed the probability distribution functions (PDFs) in eccentricity and semi-major axis of Jupiter for the 100 low accuracy and 100 high accuracy integrations. Performing a 2-sample Kolmogorov-Smirnov test finds the distributions to be statistically consistent at the 5% significance level. Small differences in the PDFs due to the accuracy of the integrator are not statistically significant. Statistical agreement between disparate integrators in Solar System dynamics has also been shown by Hernandez et al. (2020).

High accuracy symplectic integrators have a number of disadvantages compared to conventional integrators. The high accuracy symplectic integrators,

- (1) can at best only match the error behavior of conventional methods obeying Brouwer’s Law (Hairer et al. 2008; Hernandez & Holman 2021; Bartram & Wittig 2021),
- (2) do not readily accommodate adaptive stepping, which can make computation more efficient, and
- (3) unlike conventional integrators, typically assume a conservative Hamiltonian system is being solved.

Our results lead us to conclude that we can achieve a high degree of precision and accuracy in measurement of some Solar system quantities through ensembles of low accuracy integrations.

## REFERENCES

- Bartram, P., & Wittig, A. 2021, arXiv e-prints, arXiv:2102.00465. <https://arxiv.org/abs/2102.00465>
- Blanes, S., Casas, F., Farrés, A., et al. 2013, Applied Numerical Mathematics, 68, 58, doi: <https://doi.org/10.1016/j.apnum.2013.01.003>
- Duncan, M. J., Levison, H. F., & Lee, M. H. 1998, AJ, 116, 2067, doi: [10.1086/300541](https://doi.org/10.1086/300541)
- Hairer, E., Lubich, C., & Wanner, G. 2006, Geometrical Numerical Integration, 2nd edn. (Berlin: Springer Verlag)
- Hairer, E., McLachlan, R., & Razakarivony, A. 2008, BIT, 48, 231
- Hernandez, D. M., & Dehnen, W. 2017, MNRAS, 468, 2614, doi: [10.1093/mnras/stx547](https://doi.org/10.1093/mnras/stx547)
- Hernandez, D. M., Hadden, S., & Makino, J. 2020, MNRAS, 493, 1913, doi: [10.1093/mnras/staa388](https://doi.org/10.1093/mnras/staa388)
- Hernandez, D. M., & Holman, M. J. 2021, MNRAS, 502, 556, doi: [10.1093/mnras/staa3945](https://doi.org/10.1093/mnras/staa3945)
- Laskar, J., Fienga, A., Gastineau, M., & Manche, H. 2011, A&A, 532, A89, doi: [10.1051/0004-6361/201116836](https://doi.org/10.1051/0004-6361/201116836)

Laskar, J., & Robutel, P. 2001, *Celestial Mechanics and Dynamical Astronomy*, 80, 39

Rein, H., Tamayo, D., & Brown, G. 2019, *MNRAS*, 489, 4632, doi: [10.1093/mnras/stz2503](https://doi.org/10.1093/mnras/stz2503)

Wisdom, J., & Holman, M. 1991, *AJ*, 102, 1528, doi: [10.1086/115978](https://doi.org/10.1086/115978)

Wisdom, J., Holman, M., & Touma, J. 1996, *Fields Institute Communications*, Vol. 10, p. 217, 10, 217

Yoshida, H. 1990, *Physics Letters A*, 150, 262